RESEARCH ARTICLE
doi: 10.2306/scienceasia1513-1874.2022.044

ScienceAsia 48 (2022): **263–269**

Metabolite accumulation and inhibition of hypocotyl elongation by blue light induction in *Amaranthus tricolor* L.

Fang Xiao, Xiao Wang, Shengcai Liu*

Institute of Horticultural Biotechnology, Fujian Agriculture and Forestry University, Fuzhou 350002 China

*Corresponding author, e-mail: 1215698900@qq.com

Received 11 Sep 2020, Accepted 8 Jul 2021
Available online 28 Feb 2022

ABSTRACT: Red amaranth is an important fresh vegetable with valuable nutritional properties. Blue light is favorable for the accumulation of many metabolites and inhibits hypocotyl elongation in plants. However, the relation between metabolite induction and the inhibition of hypocotyl elongation by blue light in red amaranth is unclear. Here, we used LC-MS/MS-based widely targeted metabolomics to identify key compounds and to compare the metabolite composition of red amaranth under dark and blue light conditions. A total of 444 metabolites were identified, 37 of which differed between the two conditions. A pathway enrichment analysis also identified significant differences between the two conditions. Fifteen lipids, all up-regulated under the blue light, were significantly different. The amino acid content was lower under the blue light than under the dark condition. We found cyanidin chloride and anthocyanin 3-*O*-beta-D-glucoside which are the two components involved in the anthocyanin pathway. Our results verify the high nutritional quality of the red amaranth and suggest that blue light influences metabolite synthesis and hypocotyl elongation in the species.

KEYWORDS: *Amaranthus tricolor* L., blue light, metabolite profiling, hypocotyl elongation, lipids, anthocyanin

INTRODUCTION

Red amaranth (*Amaranthus tricolor* L.), a member of the family Amaranthaceae, originated in South or Southeast Asia and is widely distributed throughout warm and tropical regions worldwide [1, 2]. Among leafy vegetables, amaranth is the most commonly cultivated species. Both leaves and stems are edible. *A. tricolor* L. has nutritional value owing to its rich profile of essential metabolites, such as protein, vitamins, phenolics, flavonoids, and alkaloids [3, 4]. Fresh amaranth often provides 2 to 3 times the amount of nutrients found in other vegetables. Furthermore, medical compounds found in amaranth have broad applications as a component of complex therapies in traditional medicine in many countries [5, 6]. The nutritional value of amaranth leaves is clearly established [7]. In particular, the amino acid profile of amaranth leaves is specifically characterized by its levels of methionine and lysine [8], which are the limiting amino acids in most plants. The amaranth lipids are natural organic compounds that reduce low-density lipoprotein blood cholesterol.

Light is one of the most important and easily controllable environmental factors, and it probably influences plant metabolite profiles [9, 10]. For example, light can trigger the biosynthesis and accumulation of secondary metabolites [11]. Amongst various light spectra, blue light and red light have substantial effects on primary and secondary metabolism in plants [12]. However, blue light can be absorbed by cryptochrome in plants, which is the most operative light spectrum for the synthesis of anthocyanin and flavonoid compounds. Single-spectral blue light-emitting diodes increase anthocyanin accumulation by up-regulating the expression of anthocyanin biosynthesis genes in Chinese bayberry fruit [13]. Flavonoids are major blue light-absorbing pigments [14]. A previous report has revealed that blue light is the most effective light for promoting synthesis and accumulation of chlorogenic acid [15]. Compared with dark condition, blue light is favorable for the synthesis of betalains and carotenoids in the amaranth callus. Both metabolite synthesis and hypocotyl elongation in amaranth species were affected under blue light. However, little is known about metabolite synthesis and hypocotyl elongation inhibition by blue light in *A. tricolor* red amaranth.

Recently developed metabolomics technology provides a promising approach to reveal the physiological complexity of plants. Plant metabolomes could demonstrate comprehensive and quantitative arrays of metabolites in biological samples [16–18]. The use of mass spectrometry (MS)-based analytical platforms to identify stress-responsive metabolites associated with adaptation to adverse environmental conditions is fundamental in current plant biotechnology research programs for the development of stress-tolerant plants [19]. Liquid chromatography-tandem mass spectrometry (LC-MS/MS)-based widely targeted metabolomics is a more rapid and reliable approach compared with total scan ESI-based non-targeted metabolomics for the detection of a wide range of plant metabolites [20]. Thus, it may contribute to studies of plant systems at the molecular level, providing unbiased characteristics of total metabolite pools in plant tissues in response to environmental factors [21, 22]. In this study, we used a widely targeted metabolomics approach to identify

relevant compounds in red amaranth hypocotyls and compare the metabolite compositions under blue light and dark conditions. Our results provide basic data for the future development and utilization of amaranth.

MATERIALS AND METHODS

Plant materials

A. tricolor 'whole red' amaranth seeds were placed on plastic Petri dishes covered with three layers of wet filter paper. Seed germination was carried out under a dark condition at 25 ± 2 °C. After 5 days, half of the sample was transferred to blue light, and the other half was maintained under the dark condition for 2 days. Then, the amaranth hypocotyls were cut off for metabolite analyses.

Sample preparation and metabolite extraction

Fresh hypocotyls (1 g) were collected from amaranth seedlings and pooled to create a single biological sample. Three biological repeats were created for each treatment. All samples were stored at −80 °C until metabolite extraction. Frozen samples were freeze-dried under a vacuum and crushed using a mixer mill (MM 400; Retsch, Shanghai, China) with zirconia beads for 1.5 min at 30 Hz. Then, 100 mg of the powder sample was precisely weighed, and the extraction was done overnight at 4 °C with 1.0 ml of 70% aqueous methanol containing 0.1 mg/l lidocaine as an internal standard. Following centrifugation at 10 000 × *g* for 10 min, the supernatant was absorbed and filtered (SCAA-104, 0.22-μm pore size; ANPEL, Shanghai, China) before LC-MS/MS.

Quality control measurements

Quality control (QC) samples were prepared by mixing equal volumes of the blue light and the dark condition samples to ensure the reproducibility of the mass spectrometric results. One in ten samples was included in the QC analysis.

ESI-Q TRAP-MS/MS analysis

Extracted compounds were analyzed using an LC-ESI-MS/MS system (UPLC, Shim-pack UFLC SHIMADZU CBM30A, http://www.shimadzu.com.cn/; MS/MS, Applied Biosystems 6500 QTRAP, http://www.appliedbiosystems.com.cn/). Briefly, 2 μl of sample extract was injected onto a Waters ACQUITY UPLC HSS T3 C18 column (2.1 mm × 100 mm, 1.8 μm) operating at 40 °C and a flow rate of 0.4 ml/min. The mobile phases were acidified water (0.04% acetic acid) (Phase A) and acidified acetonitrile (0.04% acetic acid) (Phase B). Compounds were separated using the following gradient: 95:5 Phase A/Phase B at 0 min; 5:95 Phase A/Phase B at 11.0 min; 5:95 Phase A/Phase B at 12.0 min; 95:5 Phase A/Phase B at 12.1 min; and 95:5 Phase A/Phase B at 15.0 min.

The effluent was connected to an ESI-triple quadrupole-linear ion trap (Q TRAP)-MS. Linear ion trap (LIT) and triple quadrupole (QQQ) scans were acquired on a triple quadrupole-linear ion trap mass spectrometer (Q TRAP), AB Sciex QTRAP6500 System, equipped with an ESI-Turbo Ion-Spray interface, operating in a positive ion mode and controlled by Analyst 1.6.1 (AB Sciex, Singapore). The operation parameters were as follows: ESI source temperature 500 °C; ion spray voltage (IS) 5500 V; curtain gas (CUR) 25 psi; and collision-activated dissociation (CAD) set to highest. QQQ scans were acquired as MRM experiments with optimized declustering potential (DP) and collision energy (CE) for individual MRM transitions. The m/z range was set to 50–1000.

Data evaluation and metabolite identification

MS data acquisition and processing were performed as described previously [20]. The original data were preprocessed (noise filtering, peak matching, and peak extraction) and then corrected.

Metabolites were identified by searching against the self-built database MWDB (metware database, Metware Biotechnology Co., Ltd., Wuhan, China) and the public databases MassBank (http://www.massbank.jp), KNAPSAcK (http://kanaya.naist.jp/KNApSAcK), HMDB (http://www.hmdb.ca/), MoToDB (http://www.ab.wur.nl/moto/), and METLIN (http://metlin.scripps.edu/index.php). The primary and secondary spectral data were qualitatively analyzed using Analyst 1.6.1.

Multivariate statistical analysis

Unsupervised dimensionality reduction was performed by principal component analysis (PCA) for all samples using R v3.5.0 (http://www.r-project.org/). A supervised multiple regression orthogonal projection to latent structures-discriminant analysis, or orthogonal partial least-squares discriminant analysis (OPLS-DA), was performed using ropls v1.19.8 in R (http://www.r-project.org/). The OPLS-DA model was further validated by cross-validation and a permutation test ($n = 200$).

Differential metabolite analysis

Metabolites with significant differences were selected according to the variable importance in projection (VIP $\geqslant 0.8$) from the OPLS-DA model and fold change (FC $\geqslant 1.6$ or $\leqslant 0.625$) between the blue light and the dark condition samples. To assess the significance of differences in metabolite abundance, a Student's *t*-test (two-tailed) was used ($p = 0.05$). Annotated metabolites were mapped to Kyoto Encyclopedia of Genes and Genomes (KEGG) metabolic pathways for a pathway analysis and enrichment analysis. Pathways with Bonferroni corrected *p*-values of $\leqslant 0.05$ were

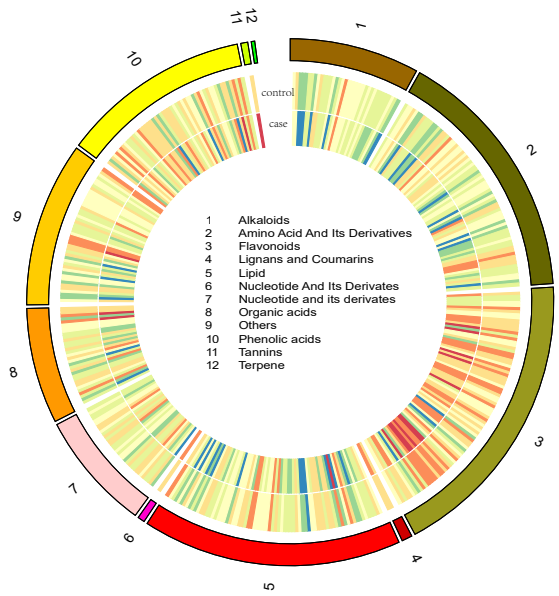

Fig. 1 Circular diagram of all metabolic components in *A. tricolor*.

considered significantly enriched. The calculated p-value was subjected to FDR correction, taking FDR $\leqslant 0.05$ as a threshold. Pathways meeting this condition were defined as significantly enriched pathways for differential metabolites.

RESULTS

Widely targeted metabolome analysis

To better understand differences of components of the 'blue' and the 'dark' samples, we performed widely targeted LC-MS/MS-based metabolite profiling. In total, 444 metabolites were identified, including 84 flavonoids, 74 lipids, 73 amino acids and derivatives, 54 phenolic acids, 37 alkaloids, 36 nucleotides and derivatives, 33 organic acids, 3 lignans and coumarins, 2 tannins, 1 terpene, and 47 other metabolites (Fig. 1 and Table S1).

Multivariate analysis of identified metabolites

The 444 metabolites were evaluated by PCA. Two principal components, PC1 and PC2, were extracted, and 37.8% and 18% of the variance were explained, respectively. The metabolites could clearly separate the two samples and the QC samples (Fig. 2A), suggesting that there were significant differences in metabolic phenotypes between the 'blue' and the 'dark' samples.

The OPLS-DA model based on the entire metabolite contents of the core samples in pairs to evaluate the differences between the blue light and the dark conditions ($R^2X = 0.791$, $R^2Y = 0.996$, $Q^2Y = 0.97$; Fig. 2B).

To eliminate the effects of quantity on pattern recognition, we performed a hierarchical cluster analysis. This analysis showed two distinct groups associated with the blue light and the dark conditions (Fig. 2C). Thus, the combination of PCA and a clustering analysis revealed distinct metabolite profiles between the 'blue' and the 'dark' samples.

The differential metabolites were screened by combining the VIP values and the fold change. We selected and compared metabolites under the dark and the blue light conditions with a fold change of $\geqslant 1.6$ (upregulated) or $\leqslant 0.625$ (downregulated). These metabolites were screened using VIP $\geqslant 0.8$ from the OPLS-DA model. In total, 37 differential metabolites were identified between the two samples (Fig. 3A and Table S1). Of these, 12 metabolites were downregulated, and 25 were upregulated in the 'blue' samples compared with the 'dark' samples (Fig. 3A). The 37 metabolites can be categorized as lipids, amino acids and derivatives, phenolic acids, organic acids, alkaloids, and nucleotides and derivatives (Fig. 3B and Table S1).

To eliminate the effects of quantity on pattern recognition, we applied a log 10 transformation of peak areas for each relative differential metabolite and performed a hierarchical cluster analysis (Fig. 4).

KEGG classification and enrichment analysis of differential metabolites

We mapped the 187 metabolites to the KEGG database. Most of the metabolites were mapped to 'Metabolism', as expected. A few metabolites were involved in 'Environmental Information Processing', 'human diseases', or 'Genetic Information Processing', suggesting that they might have health effects and confer resistance (Fig. S1). In particular, we found cyanidin chloride and anthocyanin 3-*O*-beta-D-glucoside which are the two components involved in the anthocyanin pathway (Table S1).

Subsequently, we conducted a KEGG pathway enrichment analysis to identify differences in metabolic pathways between the two samples. The enrichment analysis showed that metabolites were mainly involved in pathways related to lipids, amino acids, and the biosynthesis of other secondary metabolites (Fig. S2). The top 20 KEGG enrichment pathways were involved in the metabolism of amino acids, lipids, and so on (Fig. S3).

DISCUSSION

Amaranth is an important medicinal plant and vegetable

MS-based analytical platforms for the profiling of stress-responsive metabolites allowing plants to adapt to adverse environmental conditions are fundamental in current plant biotechnology research programs for the characterization and development of stress-

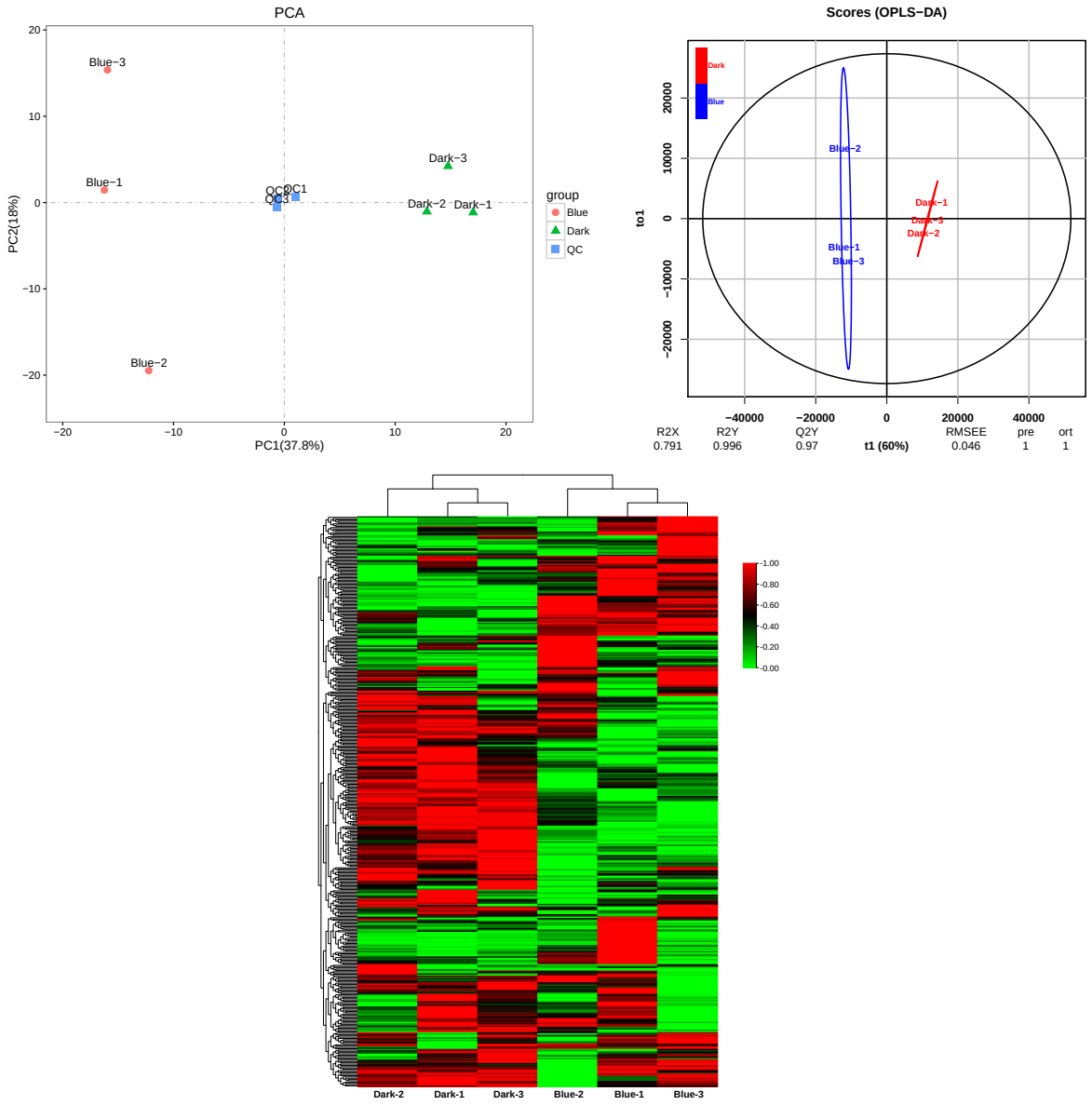

Fig. 2 Differential fruit chemotype between the 'Dark' (dark condition) and the 'Blue' (blue light) samples. (A) PCA analysis of metabolites identified from 'Dark' and 'Blue'. Equal volumes of the 'Dark' and the 'Blue' samples were mixed for use as a quality control (QC). (B) OPLS-DA score plot; and (C) Cluster analysis of metabolites from samples of 'Dark' and 'Blue'. The color indicates the level of accumulation of each metabolite, from low (green) to high (red).

tolerant plants [19]. Plant metabolomes could generate comprehensive and quantitative arrays of metabolites in biological samples [16–18].

Previous studies of metabolites in amaranth have focused on specific classes of metabolites, such as betalains (betacyanins and betaxanthin), phenolic acids, flavonoids, and alkaloids. These compounds have been isolated in various fresh plant tissues obtained at different developmental stages and/or under diverse environmental conditions [23–25]. However, the metabolic profiles of *A. tricolor* have not been thoroughly investigated. We performed LC-MS/MS-based widely targeted metabolomics to understand hypocotyls under the blue light and the dark conditions. We identified 444 metabolites, 37 of which showed differential accumulation in the 'blue' and the 'dark' samples. Thus, our results provide novel evidence for the broad application of amaranth in traditional medicine.

Flavonoids are among the most effective pharma-

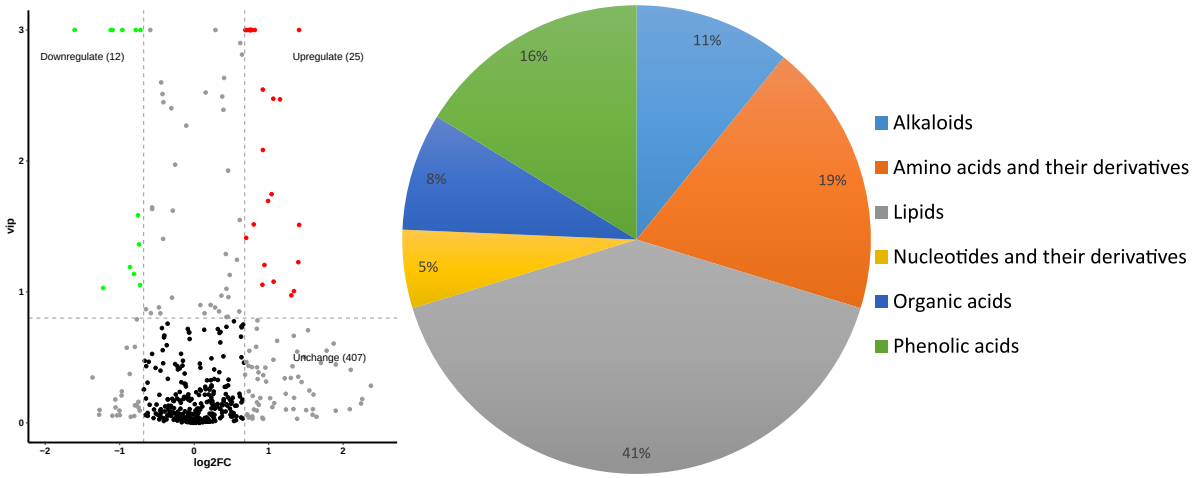

Fig. 3 Differentially accumulating metabolites between the 'Dark' and the 'Blue' Samples. (A) Volcano plot of the 444 metabolites identified; (B) Pie chart depicting the biochemical categories of the differential metabolites identified between the 'Dark' and the 'Blue' samples.

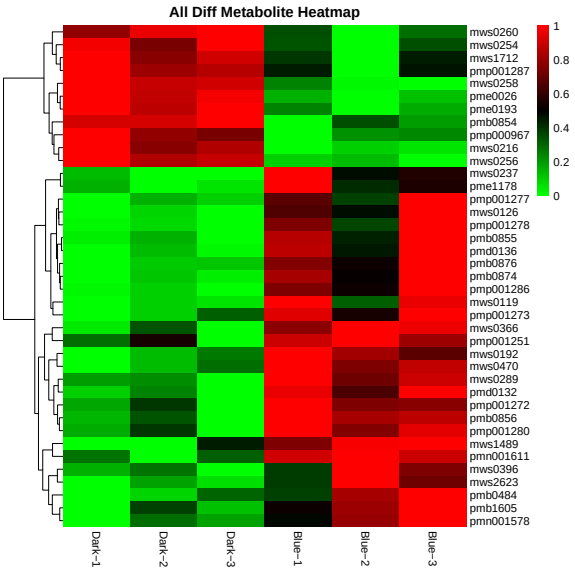

Fig. 4 Cluster analysis of differential metabolites.

cological chemicals in plants. Over 8000 flavonoids, including chalcones, flavones, flavonols, flavanones, flavanols, anthocyanins, and isoflavones have been identified. These flavonoids have various health benefits, including anti-oxidation, anti-inflammation, anti-tumor, antiviral, and antibacterial effects. Isorhamnetin, kaempferol, quercetin, and rutin were found in *A. tricolor* [26]. In the present study, from the total of 444 metabolites, 85 flavonoids, such as quercetin, naringenin, rutin, and L-epicatechin, were identified.

The compositions and abundance of amino acids are key indicators of nutritional quality. A protein content of 12–38% DM has been reported in the leaves of amaranths [27, 28]. The composition of amino acids in amaranths was similar to that of animals, with an extraordinarily high lysine content, which was 2 or 3 times higher than those in wheat or maize, respectively [29]. Previous studies have shown that *A. spinosus* contains 18 kinds of amino acids, 8 of which are essential amino acids [30]. Our widely targeted metabolomic analysis identified 73 amino acids and their derivatives, including the 18 kinds of amino acids (Table S1). This result verifies the high nutritional quality of amaranths as a very promising vegetable crop.

Lipids are natural organic compounds. The chemical and lipid compositions of amaranth seeds and oils have been studied. The oil content of amaranth seeds is predominantly unsaturated fatty acids, mainly oleic and linoleic acid [31, 32]. Furthermore, the lipid fraction contains many biologically active substances, such as tocopherols, sterols, and phospholipids, which make the amaranth oil a valuable source of useful compounds for human health [31]. Previous studies have focused on seeds; however, we performed a widely targeted metabolomic analysis of the amaranth hypocotyls. We identified 74 lipids, and 15 of which were significantly upregulated under the blue light condition.

Loss of late-acting enzymes might result in a loss of anthocyanins in amaranth

Anthocyanins are the most important flavonoids. However, they cannot coexist with betalains in the same plant [33, 34]. The transcriptional downregulation of late-acting enzymes might result in a loss of anthocyanins based on a comparative genetic study [33]. Compared to the other plants with anthocyanins, *Mirabilis jalapa* L. is lack of anthocyanins because

part of the anthocyanidin synthase (*ANS*) gene was deleted [35]. Although we found cyanidin chloride and anthocyanin 3-*O*-beta-D-glucoside which are the two components involved in the anthocyanin pathway. Hence, it is possible that the loss of late-acting enzymes results in a loss of anthocyanins in amaranth.

Blue light simultaneously affected metabolite accumulation and hypocotyl elongation

Light is one of the most important and easily controllable environment factors and is a key determinant of various metabolites and hypocotyl elongation in plants [9, 10, 36]. Among various light spectra, blue light can be absorbed by plant cryptochromes, which are photolyase-like blue-light receptors. Blue light treatment can significantly increase the expression of structural genes in plant metabolic pathways, resulting in the synthesis of secondary metabolites. In longan embryogenic calli, blue light regulates the expression of HY5, PIF4, and MYC2, thereby promoting the accumulation of rutin and catechins [37]. In citrus, blue light promotes the accumulation of carotenoids and the degradation of chlorophyll in the fruit, and some structural genes in pigment metabolism are upregulated [38–40]. Single-spectral blue light-emitting diodes increase anthocyanin accumulation by up-regulating the expression of anthocyanin biosynthesis genes in Chinese bayberry fruit [13]. These studies indicate that blue light has the potential to regulate plant secondary metabolism.

Blue light inhibits hypocotyl elongation via cryptochromes. In this study, blue light inhibited hypocotyl elongation in amaranth. We detected various metabolites, such as lipids, amino acids, and organic acids, with differences in content accumulation between the dark and the blue light samples. Interestingly, all differential lipid components showed accumulation under the blue light. This result implies that lipid metabolism plays an important role in hypocotyl elongation and metabolite synthesis in amaranth. Our results provide a novel reference for studies of the metabolism and hypocotyl elongation of amaranth under blue light and dark conditions.

CONCLUSION

A total of 444 metabolites were identified in amaranth, and 37 of which (including lipids, amino acids, and flavonoids) differed between the two samples under the blue light and the dark conditions. A pathway enrichment analysis also identified significant differences between the two conditions. Lipid metabolism plays an important role in hypocotyl elongation and metabolite synthesis in amaranth. The amino acid content was lowered. We found cyanidin chloride and anthocyanin 3-*O*-beta-D-glucoside which are the two components involved in the anthocyanin pathway. Our results verify the high nutritional quality of amaranths, as a very promising vegetable crop, and suggest that blue light influences both metabolite synthesis and hypocotyl elongation in the red amaranth.

Appendix A. Supplementary data

Supplementary data associated with this article can be found at http://dx.doi.org/10.2306/scienceasia1513-1874.2022.044. Table S1 is available from the authors upon request.

Acknowledgements: This work was supported by the Natural Science Foundation of Fujian Province (2018J01700), Excellent Master Cultivation Fund of Fujian Agriculture and Forestry University(1122YS01005), the Program for High-level University Construction of the Fujian Agriculture and Forestry University (612014028), and Rural Revitalization Service Team of Fujian Agriculture and Forestry University, China (11899170125).

REFERENCES

1. Hilou A, Ouedraogo I, Sombié P, Guenné S, Paré D, Compaoré M (2016) Leafy amaranthus consumption patterns in Ouagadougou, Burkina Faso. *Afr J Food Agric Nutr Dev* **16**, 11248–11264.
2. Li HY, Deng ZY, Liu RH, Zhu HH, Draves J, Marcone M, Sun Y, Tsao R (2015) Characterization of phenolics, betacyanins and antioxidant activities of the seed, leaf, sprout, flower and stalk extracts of three *Amaranthus* species. *J Food Compos Anal* **37**, 75–81.
3. Jiménez-Aguilar DM, Grusak MA (2017) Minerals, vitamin C, phenolics, flavonoids and antioxidant activity of *Amaranthus* leafy vegetables. *J Food Compos Anal* **58**, 33–39.
4. Arunachalam V, Dhargalkar S, Vaingankar J, Kevat N (2016) Pigment rich amaranth by tri-stimulus colorimetry and progeny test. *Natl Acad Sci Lett* **39**, 411–415.
5. Devaraj VC, Krishna BG (2013) Antiulcer activity of a polyherbal formulation (PHF) from Indian medicinal plants. *Chin J Nat Med* **11**, 145–148.
6. Yelisyeyeva O, Semen K, Zarkovic N, Kaminskyy D, Lutsyk O, Rybalchenko VK (2012) Activation of aerobic metabolism by amaranth oil improves heart rate variability both in athletes and patients with type 2 diabetes mellitus. *Arch Physiol Biochem* **118**, 47–57.
7. Peter K, Gandhi P (2017) Rediscovering the therapeutic potential of *Amaranthus* species: A review. *Egyp J Bas App Sci* **4**, 196–205.
8. Hosahatti R (2018) From zero to hero: the past, present and future of grain amaranth breeding. *Theor Appl Genet* **131**, 1807–1823.
9. Yang L, Wen K, Ruan X, Zhao Y, Wei F, Wang Q (2018) Response of plant secondary metabolites to environmental factors. *Molecules* **23**, ID 762.
10. Cai ZQ, Wang WH, Yang J, Cai CT (2009) Growth, photosynthesis and root reserpine concentrations of two *Rauvolfia* species in response to a light gradient. *Ind Crops Prod* **30**, 220–226.
11. Becker C, Klaering H-P, Schreiner M, Kroh LW, Krumbein A (2014) Unlike quercetin glycosides, cyanidin glycoside in red leaf lettuce responds more sensitively to increasing low radiation intensity before than after head formation has started. *J Agric Food Chem* **62**, 6911–6917.

12. Johkan M, Shoji K, Goto F, Hashida SN, Yoshihara T (2010) Blue light-emitting diode light irradiation of seedlings improves seedling quality and growth after transplanting in red leaf lettuce. *Am Soc Hort Sci* **45**, 414–415.
13. Shi L, Cao S, Chen W, Yang Z (2014) Blue light induced anthocyanin accumulation and expression of associated genes in Chinese bayberry fruit. *Sci Hort* **179**, 98–102.
14. Gitelson A, Chivkunova O, Zhigalova T, Solovchenko A (2017) *In situ* optical properties of foliar flavonoids: Implication for non-destructive estimation of flavonoid content. *J Plant Physiol* **218**, ID 258.
15. Narukawa M, Watanabe K, Inoue Y (2010) Light-induced root hair formation in lettuce (*Lactuca sativa* L. cv. *Grand Rapids*) roots at low pH is brought by chlorogenic acid synthesis and sugar. *J Plant Physiol* **123**, 789–799.
16. Zou S, Wu J, Shahid MQ, He Y, Yang X (2020) Identification of key taste components in loquat using widely targeted metabolomics. *Food Chem* **323**, ID 126822.
17. Wang X, Bai J, Wang W, Zhang G, Wang D (2021) A comparative metabolomics analysis of the halophyte *Suaeda salsa* and *Salicornia europaea*. *Environ Geochem Health* **43**, 1109–1122.
18. Gao J, Ren R, Wei Y, Jin J, Zhu G (2020) Comparative metabolomic analysis reveals distinct flavonoid biosynthesis regulation for leaf color development of Cymbidium sinense 'Red Sun'. *Int J Mol Sci* **21**, ID 1869.
19. Jorge TF, Rodrigues JA, Caldana C, Schmidt R, António C (2016) Mass spectrometry-based plant metabolomics: Metabolite responses to abiotic stress. *Mass Spec Rev* **35**, 620–649.
20. Chen W, Gong L, Guo Z, Wang W, Zhang H, Liu X, Yu S (2013) A novel integrated method for large-scale detection, identification, and quantification of widely targeted metabolites: application in the study of rice metabolomics, *Mol Plant* **6**, 1769–1780.
21. Ziran W, Yuanyuan C, Alexander V, Shangwu C, Huiqin M (2017) Regulation of Fig (*Ficus carica* L.) fruit color: metabolomic and transcriptomic analyses of the flavonoid biosynthetic pathway. *Front Plant Sci* **8**, ID 1990.
22. Dandan W, Liangxiao Z, Xiaorong H, Xiao W, Ruinan Y, Jin M, Xuefang W, Xiupin W, et al (2018) Identification of nutritional components in black sesame determined by widely targeted metabolomics and traditional Chinese medicines. *Molecules* **23**, ID 1180.
23. Miguel MG (2018) Betalains in some species of the Amaranthaceae family: a review. *Antioxidants* **7**, ID 53.
24. Karamac M, Gai F, Longato E, Meineri G, Janiak M, Amarowicz R, Peiretti PG (2019) Antioxidant activity and phenolic composition of amaranth (*Amaranthus caudatus*) during plant growth. *Antioxidants* **8**, ID 173.
25. Liu S, Zheng X, Pan J, Peng L, Cheng C, Wang X, Zhao C, Zhang Z, et al (2019) RNA-sequencing analysis reveals betalains metabolism in the leaf of *Amaranthus tricolor* L. *PLoS One* **14**, e0216001.
26. Srivastava R (2017) HPTLC fingerprint analysis of herbs with nutraceutical potentials: *Amaranthus tricolor* and *Amaranthus viridis*. *Pharm Innov* **6**, 324–327.
27. Tunick MH, Elvira GDM (2006) Amaranth: an ancient crop for modern technology. *Acs Symp* **946**, 103–116.
28. Andini R, Yoshida S, Ohsawa R (2013) Variation in protein content and amino acids in the leaves of grain, vegetable and weedy types of amaranths. *Agronomy* **3**, 391–403.
29. Zheleznov AV, Solonenko LP, Zheleznova NB (1997) Seed proteins of the wild and the cultivated *Amaranthus* species. *Euphytica* **97**, 177–182.
30. Puqing Z (1998) Content of amino acids in *Amaranthus Spinosus* and its nutritional Evaluation. *Amino Acids Biotic Resour* **4**, 41–42.
31. Tang Y, Li X, Chen PX, Zhang B, Liu R, Hernandez M, Draves J, Marcone MF, et al (2016) Assessing the fatty acid, carotenoid, and tocopherol compositions of amaranth and quinoa seeds grown in Ontario and their overall contribution to nutritional quality. *J Agric Food Chem* **64**, 1103–1110.
32. Petkova ZY, Antova GA, Angelova-Romova MI, Vaseva (2019) A comparative study on chemical and lipid composition of amaranth seeds with different origin. *Bulg Chem Commun* **51**, 262–267.
33. Brockington SF, Walker RH, Glover BJ, Soltis PS, Soltis DE (2011) Complex pigment evolution in the Caryophyllales. *New Phytol* **190**, 854–864.
34. Harris NN, Javellana J, Davies KM, Lewis DH, Jameson PE, Deroles SC, Calcott KE, Gould KS, et al (2012) Betalain production is possible in anthocyanin-producing plant species given the presence of DOPA-dioxygenase and L-DOPA. *BMC Plant Biol* **12**, ID 34.
35. Polturak G, Heinig U, Grossman N, Battat M, Leshkowitz D, Malitsky S, Rogachev I, Aharoni A (2018) Transcriptome and metabolic profiling provides insights into betalain biosynthesis and evolution in *Mirabilis jalapa*. *Mol Plant* **11**, 189–204.
36. Coelho GC, Rachwal MFG, Dedecek RA, Curcio GR, Nietsche K, Schenkel EP (2007) Effect of light intensity on methylxanthine contents of *Ilex paraguariensis* A. St. Hil. *Biochem Syst Ecol* **35**, 75–80.
37. Li H, Lyu Y, Chen X, Wang C, Lai Z (2019) Exploration of the effect of blue light on functional metabolite accumulation in longan embryonic calli via RNA sequencing. *Int J Mol Sci* **20**, ID 441.
38. Zhang L, Ma G, Yamawaki K, Ikoma Y, Matsumoto H, Yoshioka T, Ohta S, Kato M (2015) Effect of blue LED light intensity on carotenoid accumulation in citrus juice sacs. *J Plant Physiol* **188**, 58–63.
39. Yuan Z, Deng L, Yin B, Yao S, Zeng K (2017) Effects of blue LED light irradiation on pigment metabolism of ethephon-degreened mandarin fruit. *Postharvest Biol Technol* **134**, 45–54.
40. Deng L, Yuan Z, Xie J, Yao S, Zeng K (2017) Sensitivity to ethephon degreening treatment is altered by blue LED light irradiation in mandarin fruit. *J Agric Food Chem* **65**, 6158–6168.

Appendix A. Supplementary data

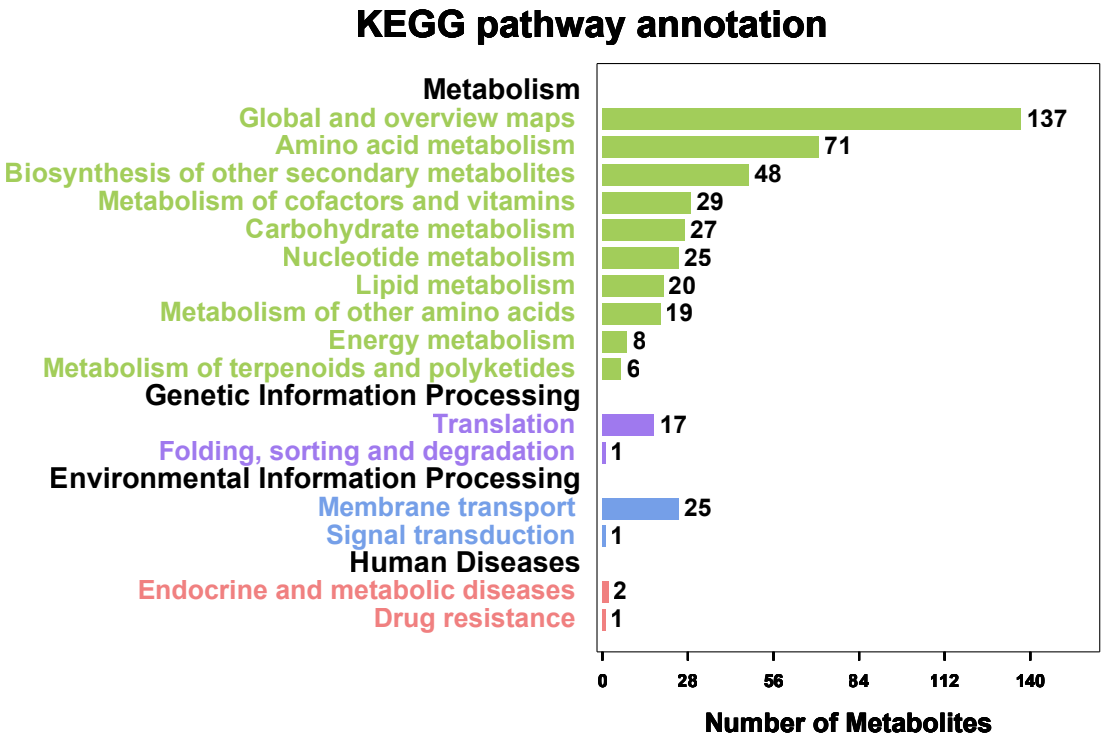

Fig. S1 KEGG classification of all metabolites.

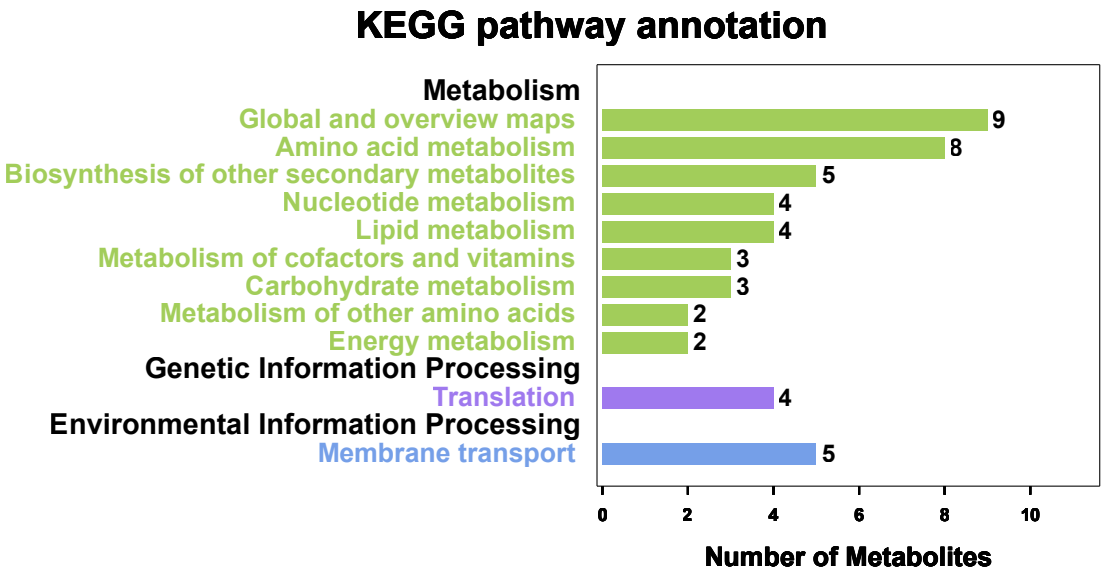

Fig. S2 KEGG classification of differential metabolites.

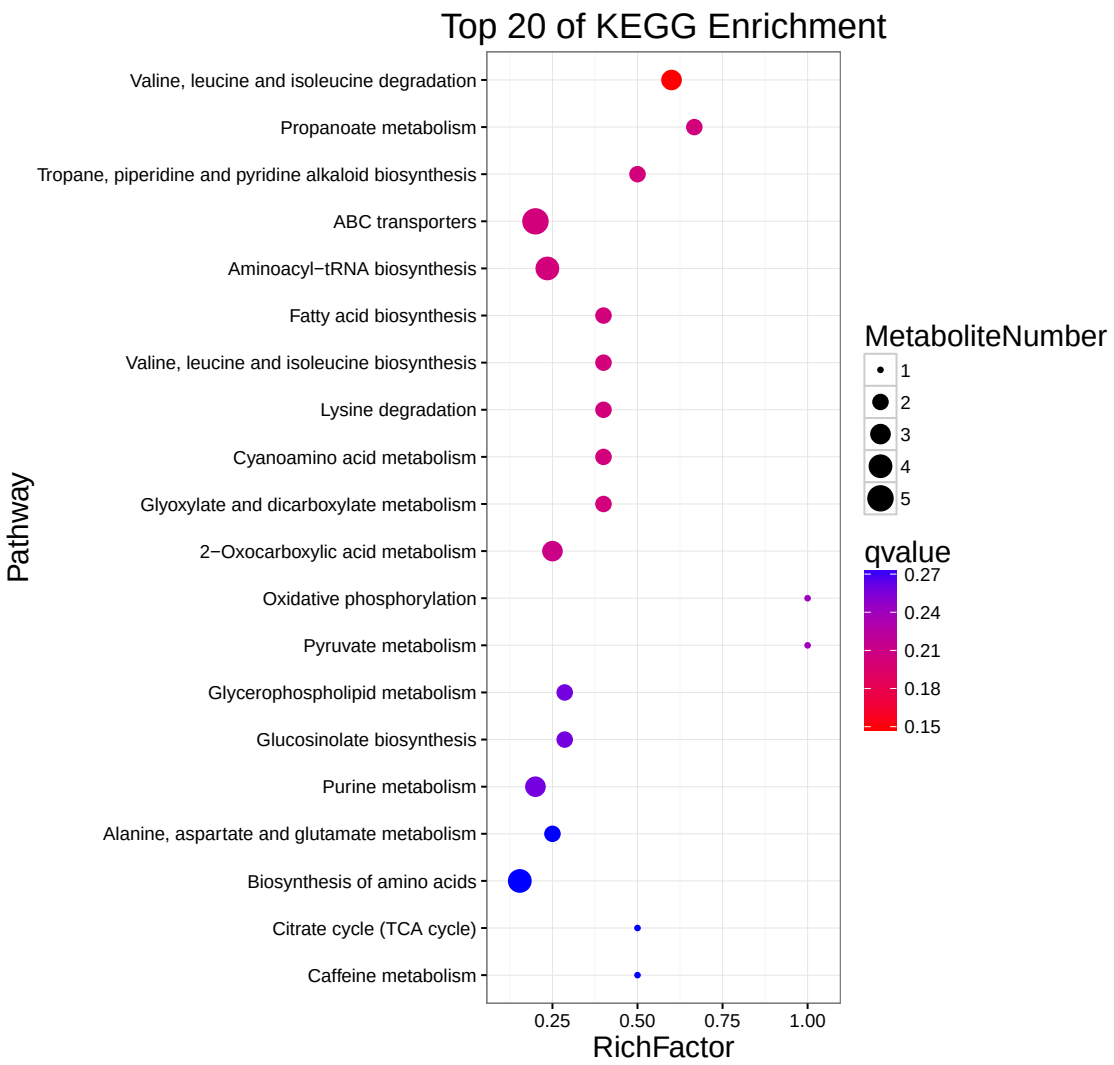

Fig. S3 Top 20 of KEGG enrichment.